



From left to right, back row: K. Brown, S. Labouré, L. Claustre, R. Pinck. Back row: G. Leonard, V. Biou, F. Lapeyre, A. Thompson, V. Stojanoff, M. Mattenet, F. Felisaz.

GOING MAD ON BM14

V. BIOUS¹, G. LEONARD², V. STOJANOFF²,
S. LABOURÉ², M. MATTENET²,
J. HELLIWELL³, F. FELIZAZ⁴, L. CLAUSTRE⁴,
F. LAPEYRE⁴, K. BROWN⁴
AND A. THOMPSON⁴

1 IBS AND ESRF, GRENOBLE (FRANCE)

2 ESRF, EXPERIMENTS DIVISION

3 UNIVERSITY OF MANCHESTER (UK)

4 EMBL, GRENOBLE OUTSTATION (FRANCE)

BM14 supplies a narrow bandpass, rapidly tunable source of intense X-rays for structure determination using Multi-Wavelength Anomalous Diffraction (MAD) from macromolecular crystals, and was built as a collaboration between the EMBL and the ESRF.

The MAD method has been extensively developed by Hendrickson, and his excellent review [1] gives an overview of the field as it was in 1991. For a more recent review, see Fourme et al [2].

Over the last 18 months on the beamline a number of new structures have been solved either using «pure» MAD phasing, or by incorporating phase information from elsewhere. These have, in the main, been solved using a MAR research image plate detector, which produces excellent quality data but has a readout time which is slow compared to the sample exposure times used on the beamline. To alleviate this problem, work has progressed towards the calibration [3] and usage of an Image Intensified CCD detector (II/CCD) developed at the ESRF by J.-P. Moy of the detector group [4], and resulted in several successful data collections with the detector, and the solution of a new structure by MAD phasing using the detector.

The French Collaborating Research Group beamline (D2AM) has also successfully used MAD to solve new protein structures.

BM14 has been operational since September 1995.

The bandpass with the replacement monochromator crystal currently available is approximately 2.5×10^{-4} from a Si(111) monochromator. A Si(311) monochromator and a second Si(111) monochromator with an

improved surface finish are available for testing early in 1997. Wavelength is rapidly tunable between limits of 0.6 Å and 1.8 Å - the wavelength can be accurately and reproducibly changed within these limits within a few minutes.

MAD, AND HOW TO DO IT

One of the major barriers to resolving a macromolecular crystal structure is the solution of the phase problem, i.e. the reconstruction of the phase of the diffracted X-rays. The most common method of doing this is by using Multiple Isomorphous Replacement (MIR), i.e. by producing «heavy atom derivatives» of the crystal which are «isomorphous» or identical in terms of the arrangement of

molecules inside the crystal. More recently the MAD method (Hendrickson [1]) has become increasingly popular in deriving phases, and offers significant advantages over other methods.

The great advantage of the MAD method is that it does not depend on crystal isomorphism. «Isomorphous» derivatives are rarely completely so, and tend to look worse when the crystal structure is examined in higher detail (ie at higher resolution). In principle, MAD can therefore provide better measurements of phase to higher resolution (if the crystals diffract sufficiently well). In addition, the anomalous signal depends to a lesser extent on diffraction angle than the normal scattering, so that it should (in theory at least) become more significant at higher resolution.

Table 1:
Likely «heavy atom» targets for MAD measurements. Most elements with Z > 24 are suitable if they contribute sufficient anomalous signal (see Equation).

Category	Anomalous scatterer
Metalloproteins	
Transition metals	Fe, Cu, Zn, Mn
Other metals	Ca, Mo
Metal replacements	
Lanthanides for Ca ²⁺ , Mg ²⁺	Tb, Ho, Yb
Mercury for Zn	Hg
Heavy atom complexes	
Common protein derivatives	Pt, Au, Hg, Pb, W, U
Cluster compounds	Ta, W
Building - unit analogs	
Selenomethionine or selenocysteine	Se
Telluromethionine	Te
Brominated or iodinated nucleotides	Br, I

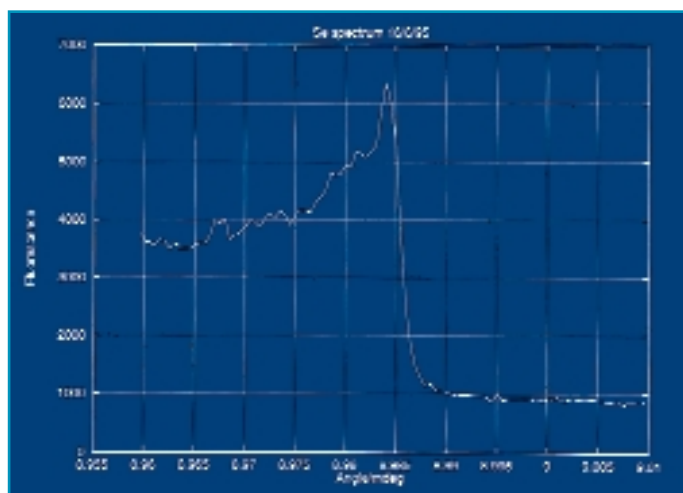


Briefly, protein crystals can naturally contain or have incorporated within them «heavy atom» scatterers (see Table 1, based on Hendrickson [1]) which exhibit anomalous scattering in the X-ray region (the bulk of the atoms making up a large protein structure being carbons, nitrogens and oxygens, which exhibit no anomalous scattering in the X-ray region). Heavy atom incorporation is discussed in Pappa et al [4].

If the energy of the incident X-ray beam is close to the energy of an electron transition from an inner bound state to a higher state or the continuum of states, there results both an absorption of the incident X-rays and a resonance in sympathy with the natural frequency of the bound electron, which peaks when the incident X-ray energy is identical to the energy required for the (quantum mechanically allowed) transition. This in turn modifies the overall contribution of the «heavy atom» to each diffraction spot, and gives rise to «anomalous» differences between intensities of mirror plane related reflections (Bijvoet pairs) recorded at any one wavelength, and «dispersive differences» between the same reflection measured at different wavelengths. The information from the anomalous differences can be used to locate the «heavy atom» in the unit cell, and the combined information from the anomalous and dispersive differences can be used to calculate a unique phase for each reflection and hence «solve» the crystal structure.

A MAD experiment therefore consists of measuring the absorption (or more

Fig. 1: Typical fluorescence spectrum from a Se-met protein crystal.



frequently, fluorescence) spectrum of the «heavy atom» as a function of incident X-ray energy, and collecting several X-ray diffraction data sets at energies chosen to maximise both the anomalous and dispersive signals. Figure 1 shows a typical fluorescence spectrum from a protein crystal (in this case a class II aldolase, modified to contain Se instead of S in methionine residues, Hunter [6]).

Unfortunately the size of these signals is small, often only a few percent, and is given by (Smith [7]) :-

$$\Delta_{anom} = \sqrt{\frac{N_{anom} 2f_{max}''}{2 \langle |F_p| \rangle}}$$

$$\Delta_{disp} = \sqrt{\frac{N_{anom} |f_{max}' - f_{max}''|}{2 \langle |F_p| \rangle}}$$

where $\langle |F_p| \rangle$ is the total scattering due to the molecule, f_{max}'' is the maximum

«anomalous» scattering component arising from the absorption of X-rays, f_{λ_i}' is the «dispersive» or resonant component at wavelength «i», N_{anom} is the number of anomalous scatterers per molecule, and Δ_{anom} and Δ_{disp} refer to the maximum anomalous and dispersive intensity differences expected as a fraction of the overall scattering. Note that these expressions only apply when there is a single species of anomalous scatterer present, and the anomalous scattering is a small fraction of the overall scattering. For those wishing to make these calculations to test the feasibility of their own MAD experiment, values of f' and f'' can be found in (for example) Sasaki [8]. The behaviour of these quantities around an X-ray absorption edge are indicated in Figure 2, which also shows how «normal» and «anomalous» scattering adds to give the overall «observable» structure factor.

Fig. 2: a) A theoretical Se absorption spectrum. The f' value is always negative in the diagram, and reaches a minimum at the absorption edge. b) An Argand diagram showing how F_{obs} , the «observable» structure factor is made up of the scattering due to the anomalous scatterer F_A , F_A' and F_A'' . F_P is the scattering due to the rest of the atoms in the protein.

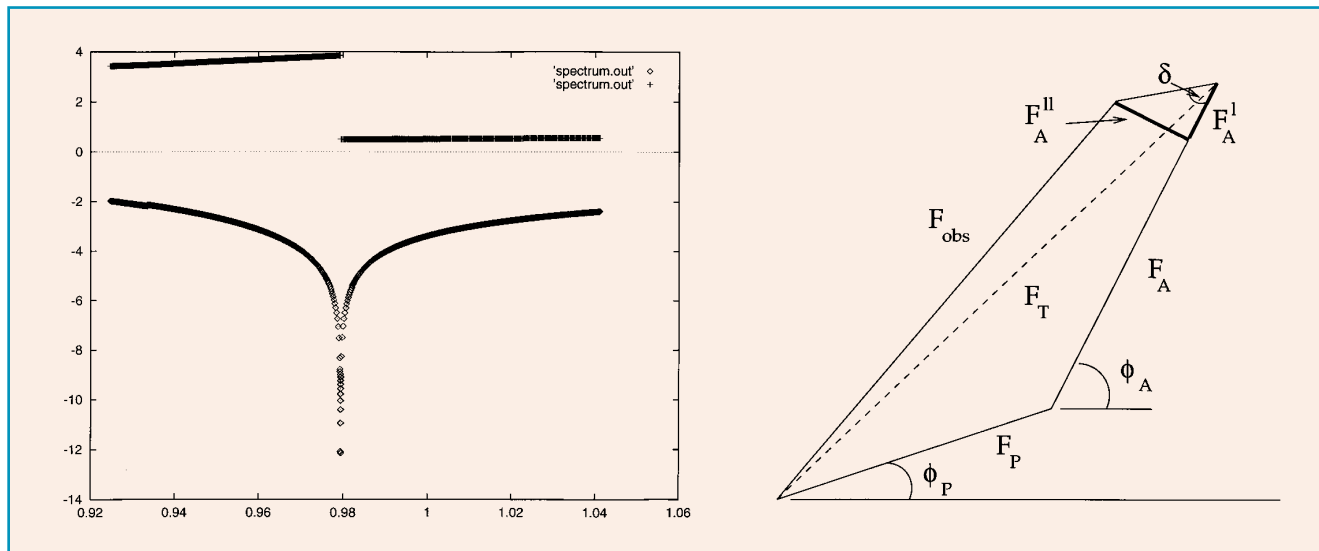




Table 2 gives values of the expected maximum anomalous and dispersive differences for a «typical» case of a 30 kDa molecule with various anomalous scatterers. Since these signals are small (often comparable with the intrinsic accuracy of diffraction data), care has to be taken in their measurement.

In particular :

- If Bijvoet related reflections are measured close together in time (ideally on the same image) systematic errors due to variation of the intensity of the incident X-ray beam, variation of the exposure time due to a faulty X-ray shutter, sample radiation damage, etc. are eliminated hence giving an accurate measurement of the anomalous differences. This requires alignment or «setting» of the crystal in a particular orientation, and is not always possible due to the morphology of the sample or a limitation in the beamline goniometer. In this latter case, data can be collected in «inverse beam geometry» or by rotating the crystal to view the Bragg planes in the opposite sense and hence record Bijvoet mates in successive images (but still close together in time).

The stability of modern synchrotron sources such as the ESRF, and the cryo - protection of samples which greatly slows down radiation damage, considerably reduces systematic errors in the data so that very accurate alignment of the sample is not always necessary (a great simplification of data collection procedures).

- Since the signal is small, care must be taken to minimise measurement noise

Anomalous scatterer	NO of scatterers	Percentage anomalous difference
Pt	1	4.7
Se	1	1.8
Se	4	3.5
Hg	1	4.3
Yb	1	4.9

Table 2: Theoretical maximum anomalous signals at the peak of the absorption edge. Note that scatterers that exhibit a «white line» (for example Se in Se-met) have an amplified anomalous effect. Signals below 3 % are very hard to measure unless X-ray data is of excellent quality.

(X-ray background, electronic noise from area detectors) and counting time must be increased to give a signal with sufficient statistical accuracy to discriminate between the normal and anomalous scattering. In the case of weak, high resolution diffraction spots, this often entails collecting data twice at different X-ray exposures, or by «extending» the detector dynamic range by using absorbers to weaken the low resolution diffraction pattern (or buying a higher dynamic range detector!)

- The structure is calculated from a knowledge of the intensity and phase of all reflections. Therefore care must be taken not only to measure «complete» data, but also to measure all Bijvoet pairs. This can be easily achieved by the use of a suitable prediction program, such as the STRATEGY option of MOSFLM (Leslie). It is wise to have sufficient redundancy in the data to be able to distinguish between good measurements of intensity and those subject to error due to being close to spurious detector «events» (ice rings, zingers, dirty thumb prints etc).

A RECENT MAD STRUCTURE

The structure of Maclura Pommifera Agglutinin (a moraceae plant lectin) is of great medical interest due to its high affinity and specificity to bind tumour specific molecules, antigens, on the surface of carcinoma cells (Table 3) from which 85% of cancers develop. This structure was solved in collaboration with a group from the Department of Cancer Biology (Cleveland Cancer Research Clinic) protein crystallography laboratory headed by Dr X. Lee, and was the first MAD structure to be solved on BM14 using the II/CCD detector.

Details of the crystal and molecule are given in Table 4. Although the protein is itself rather small (153 or 154 amino acid residues), structure solution was not easy due to the great difficulty in finding isomorphous derivative crystals. A possible Pb containing crystal was found to give a strong fluorescent spectrum on the beamline. Hence three datasets were collected spanning the lead absorption edge. Figure 3 shows the anomalous and dispersive Pattersons from data collected close to the absorption edge, demonstrating quite clearly the high data quality and stability of the II/CCD detector. MAD phasing proceeded by finding the Pb atoms by solving the Patterson map (two high-occupancy sites

Intradermal delayed-type hypersensitivity response to erythrocyte-derived T-antigen (DTHR-T), at initial visit, of carcinoma patients and controls.

Category	DTHR-T+/total tested
Lung	
Carcinoma	
Adeno	45/49
Brochioloalveolar	5/6
Small-cell	15/17
Squamous-cell	12/14
Large-cell anaplastic	1/1
Other pleuropulmonary cancers	1/5
Benign diseases	2/35
Pancreas	
Adenocarcinoma	23/26
Pancreatitis	0/13
Breast adenocarcinoma	
Ductal	
Stage I noninfiltrating	10/12
Stage I infiltrating	32/37
Stage II and III	37/42
Stage IV	17/17
Total	96/108

Table 4: Crystal parameters for MPA.

MPA & p-hydroxymercuriphenyl sulfonic acid

Space group: C222.

Cell parameters:

$a = 58.97 \text{ \AA}$, $b = 119.5 \text{ \AA}$ and $c = 155.41 \text{ \AA}$

Two molecules of $(a + b)$ per asymmetric unit.

Crystallization conditions: hanging drop method.

Reservoir solution:

0.5 M Li_2SO_4 and 7.5 %

PEG 8000 plus 1 %

octyl- β -D-glucopyranoside (O.G.).

Table 3: Specificity of MPA to T-Antigen binding.

easily identified), and scaling and phasing the data using programs in the CCP4 [9] program suite (SCALEIT and MLPHARE). The phasing statistics were «encouraging», the overall figure of merit being 69% to 2.9Å resolution, and the map quality excellent. The high quality of the map was perhaps unsurprising given the modest size of the protein and the large anomalous signal from the two Pb atoms. The protein was traced using a solvent flattened map (DM, cowtan). The model was then used to find a molecular replacement solution for data collected from crystals with the tumour antigen Gal β ,3GalNAc bound (data to 2.2 Å resolution collected at the Cleveland Cancer Research Clinic using a rotating anode). The current refined model, showing the antigen bound, is shown in Figure 4.

MAD maps can often be of high quality if the data collected is complete, even for cases where the anomalous signal is «more typical» i.e. lower! The protein ALA dehydratase, studied for the last 6 years by Dr J. Cooper of Birkbeck College, London, is extremely difficult to derivatise, and certain metals (for example Pb) inhibit the protein. The protein itself, however, contains five methionine residues in a 38 kDa molecular weight, so biological substitution of selenium for sulphur provided an alternative approach to obtaining phase information (as suggested by Hendrickson [10]). A MAD

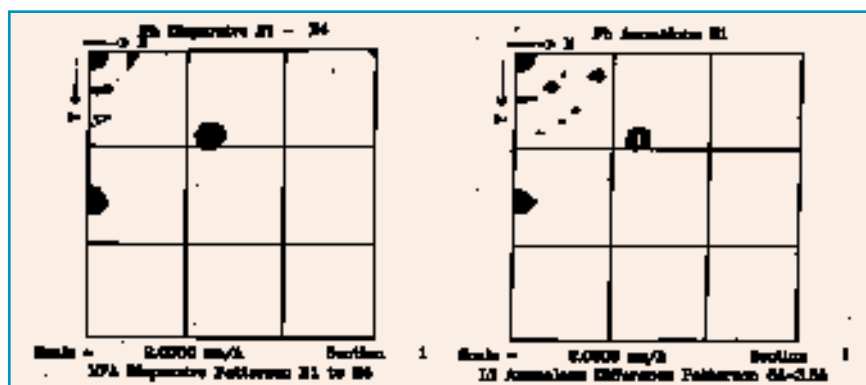


Fig. 3: Zeroeth «w» sections of the anomalous and dispersive Pattersons, contoured in 0.5 sigma intervals with a cutoff of 2 sigma.

experiment was performed using the selenated form of the protein, yielding an extremely good electron density map which was phase extended to 2.5 Å resolution. The data were collected from a randomly oriented crystal using a MAR image plate (loaned from the EMBL), and phases calculated using MLPHARE [9]. The overall figure of merit was 62%, with an overall phasing power of 1.3 and Cullis factor of 0.69 (to 3.5 Å). Figure 5 shows a section of alpha helix from the solvent flattened map, illustrating the extremely high quality of the electron density map.

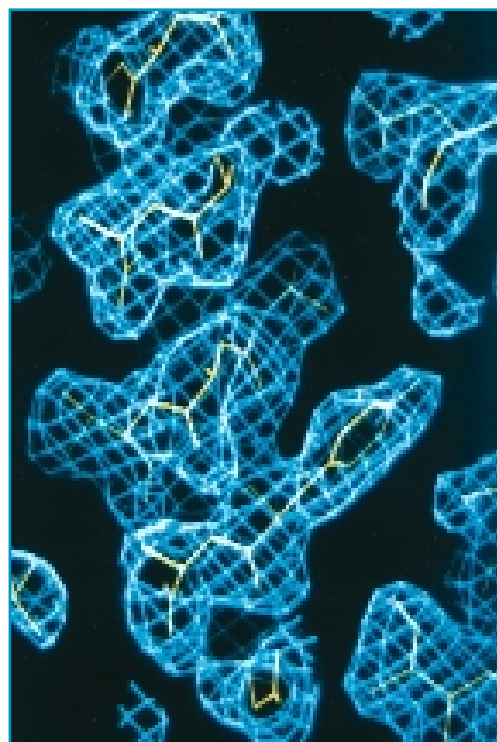
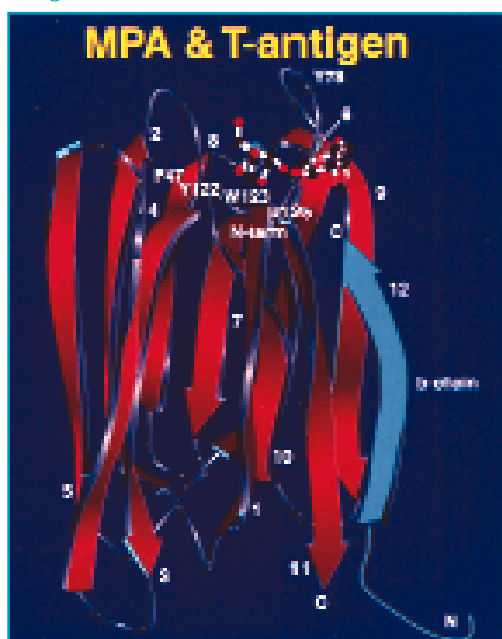


Fig. 5: A portion of an alpha-helix form the «MAD» electron density map of ALAD (courtesy of J. Cooper).

Fig. 4: Current model of MPA with T-antigen bond.



SOME TECHNICAL DEVELOPMENTS

Significant technical progress has also been made on the beamline, with the first experiments being performed with the rapid image plate changer – a device capable of changing an exposed plate in 0.15 s. Figure 6 shows a plate being mounted on the new system. The image plates themselves are identified by a bar code reader both as they are exposed in the X-ray beam and just before reading in the FUJI BAS2000 image plate scanner. Details of the oscillation angle of the exposure, wavelength,

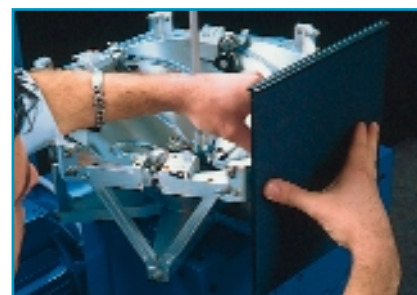


Fig. 6: Mounting an image plate on the rapid plate changer.

time of exposure, etc. are recorded in a data base which can be displayed using a network browser. The knowledge of the time elapsed between exposure and reading of the plate permits a correction to be made for the decay of the photo stimulated luminescence. A test experiment was performed using this



detector and crystals of ribonucleotide reductase (RNR, a known structure studied in the laboratory of P. Nordlund at the University of Stockholm). RNR will not crystallise in the absence of Hg, and can contain up to 10 Hg binding sites in a protein of 530 amino acids. Hence the anomalous signal is potentially very large and a MAD experiment feasible. The crystals diffract to high resolution. Three wavelengths of data were collected around the Hg absorption edge and inspection of

has been modified in order to collect data using the beamline goniostat and the II/CCD detector. A graphical user interface PXGEN (Kinder [13]) developed at the PPSRC Daresbury Laboratory, UK, allows easy control of data collection, and has recently been installed for testing on the beamline.

WORKING WITH MAD

In order to further promote the MAD technique, a study week was arranged in Grenoble in June 1996 to discuss and teach the method to scientists from Europe, the USA and Japan. Demand for places exceeded availability by a ratio 3:1, so that many good applicants had to be rejected. Hence a second MAD Practical Course will be held in Grenoble in June 1997, this time with funding from the European Molecular Biology Organisation.

CONCLUSION

MAD phasing is now an extremely important tool with which X-ray crystallographers can solve the «phase problem» to reveal the internal folding of protein structures of great biological interest. The additional intensity and stability of the ESRF beam provides an excellent facility for the exploitation of this technique in Europe. This improvement will be further consolidated when an undulator beamline for MAD protein crystallography (Shapiro et al [14], Biou et al [15]) becomes available at the ESRF in 1999, which should give a tenfold intensity gain enabling more and more complicated structures to be solved using the MAD method. ■

References

- [1] W. A. Hendrickson, *Science* 254 (1991) pp 51 - 58.
- [2] R. Fourme, W. Shepard and R. Kahn, *Progress in Biophysics and Molecular Biology* 64 (1996) pp 167 - 199.
- [3] A. P. Hammersley, S. O. Svensson, J.-P. Moy, A. Gonzalez, K. Brown, W. Burmeister, S. McSweeney, A. Thompson,



Fig. 7: Section of the electron density map of RNR showing one of the two Fe sites (courtesy of P. Nordlund).

accepted for publication in *Journal of Synchrotron Radiation* (1997).

[4] J.-P. Mo., *Nuclear Instruments and Methods A* 346 (1994) pp 641 - 644.

[5] H. S. Pappa, A. E. Stewart and N. Q. McDonald, *Current Opinion in Structural Biology* 6 (1996) 611 - 616.

[6] S. J. Cooper, G. A. Leonard, S.M. McSweeney, A.W. Thompson, J.H. Naismith, S. Qamar, A. Plater, A. Berry and W. N. Hunter., *Structure* 4 (1996) pp 1303 - 1315.

[7] J. L. Smith, *Current Opinion in Structural Biology* 1 (1991) pp 1002 - 1011.

[8] S. Sasaki, KEK Report 88-14 (1989), National Laboratory for High Energy Physics, Tsukuba, Japan.

[9] CCP4, *Acta Crystallographica D* (1994) pp 760 - 763.

[10] W. A. Hendrickson, *Transactions of the American Crystallographic Association* 21 (1985) pp 11 - 21

[11] R. J. Reed, *Structure* 4 (1996) pp 11 - 14.

[12] A. Messerschmidt and J. W. Pflugrat, *Journal of Applied Crystallography* 20 (1987) pp 306 - 315.

[13] S. H. Kinder, S. M. McSweeney and E. M. H. Duke, *Journal of Synchrotron Radiation* 3 (1996) pp 296 - 300.

[14] L. Shapiro, A. M. Fannon, P. D. Kwong, A. Thompson, M. S. Lehmann, G. Grübel, J.-F. Legrand, J. Als-Nielsen, D.R. Colman and W. A. Hendrickson, *Nature* 374 (1995) pp 327 - 337.

[15] V. Biou, A. Gonzalez, J. R. Helliwell, S. McSweeney, J. L. Smith and A. Thompson, Report to the ESRF Science Advisory Committee (1995).

Dataset	Site n°	Occupancy	
		Dispersive	Anomalous
L1	1	8.266	10.112
	2	8.521	8.745
	3	7.987	9.830
	4	6.943	8.828
	5	3.502	3.821
	6	3.158	3.628
	7	1.972	2.206
L3	1	2.639	10.328
	2	1.743	8.553
	3	2.813	10.141
	4	2.823	9.052
	5	0.606	3.652
	6	0.654	3.411
	7	0.375	0.040
L2	1	0.000	7.123
	2	0.000	5.902
	3	0.000	6.748
	4	0.000	6.327
	5	0.000	2.527
	6	0.000	2.460
	7	0.000	1.363

Table 5: Site occupancies after refinement.

the Patterson map calculated at the peak of the Hg absorption edge yielded seven sites of varying occupancy.

Table 5 shows the occupancy of the various Hg sites (refined from the program MLPHARE [9]). These sites were used to calculate phases to high (2.0 Å) resolution, a typical section of electron density being shown in Figure 7. The impact of collecting MAD data to high resolution is discussed in Reed [11].

Other new technical developments on the beamline include the new crystal mounting laboratory and data processing room adjoining the beamline, a joystick for quick and easy sample alignment, and improved cryogenic facilities for freezing, storing and transferring crystals to the X-ray beam.

The program MADNES [12] for collecting and analysing data collected with a diffractometer and area detector,